J Nonlinear Sci
DOI 10.1007/s00332-012-9133-6

Journal of Nonlinear Science

Mass Structured Systems with Boundary Delay: Oscillations and the Effect of Selective Predation

O. Angulo · J.C. López-Marcos · M.A. Bees

Received: 10 November 2011 / Accepted: 15 May 2012

Abstract We study equilibrium and oscillatory solutions of a general mass structured system with a boundary delay. Such delays may be derived from systems with a separate egg class. Analytical calculations reveal existence criteria for non-trivial steady states. We further explore parameter space using numerical methods. The analysis is applied to a typical mass structured slug population model revealing oscillations, pulse solutions and irregular dynamics. However, robustly defined isolated cohorts, of the form sometimes suggested by experimental data, do not naturally emerge. Nonetheless, disordered, leapfrogging local maxima do result and may be enhanced by selective predation.

Keywords Structured population model · Numerical integration · Slugs · Characteristics · Oscillations · Leapfrogging

Communicated by Philip K. Maini.

O. Angulo (✉)
Departamento de Matemática Aplicada, ETSIT, Universidad de Valladolid Pso Belén, 15, 47011 Valladolid, Spain
e-mail: oscar@mat.uva.es

J.C. López-Marcos
Departamento de Matemática Aplicada, Facultad de Ciencias, Universidad de Valladolid, C/Prado de la Magdalena, s/n, 47005 Valladolid, Spain
e-mail: lopezmar@mac.uva.es

M.A. Bees
Department of Mathematics, University of Glasgow, Glasgow G12 8QW, UK
e-mail: Martin.Bees@glasgow.ac.uk

Published online: 21 June 2012

Mathematics Subject Classification 22E46 · 53C35 · 57S20 · 65P40

1 Introduction

Motivated by an application in modelling gastropod populations and associated biological control issues (Rae et al. 2007), we shall investigate a general continuous mass structured system with a simple boundary delay that can represent a distinct egg class, or a similar dynamically isolated life-stage. This analysis is part of a larger study to explore mechanisms that generate distinct structured population classes with regard to the mass of individuals, which we shall call cohorts. Whilst we preserve the generality of the equations in the stability analysis, for numerical specificity we consider an example slug population system (Bees et al. 2006), where the masses of individuals range over two orders of magnitude.

Experimental data on slug populations suggest that

1. distinct cohorts have been observed (groups of individuals with similar mass or age; but the degree of overlap between cohorts is unclear),
2. leapfrogging generations naturally arise (Hunter and Symmonds 1971; such that a cohort of mature adults gives rise to a batch of eggs, neither of which are directly related to an intermediate cohort of juveniles nor an immediately older cohort), and
3. irregular (and perhaps chaotic) total biomass dynamics are recorded for the generally dominant species *Deroceras reticulatum* (e.g. South 1989, 1992, hypothesised to be associated with its competitive edge, Schley and Bees 2003).

In contrast, numerical analyses of mass structured slug dynamics have previously only yielded stable equilibrium states. Thus it is natural to ask whether oscillatory solutions exist and, if so, whether they posses a form accordant with experimental evidence. If time dependent solutions do not occur robustly from the standard dynamics then alternative mechanisms must be sought for oscillatory solutions. Suitable candidates are (A) more complex dynamics, such as explicit predator-prey interactions, (B) spatial structure, and (C) external (e.g. seasonal) forcing of the system that may amplify pulse-like transients (see discussion).

Here, we shall investigate an autonomous system (i.e. one not driven by seasonal forcing). In particular, we shall analytically determine exact conditions for the existence of a steady state, and shall explore bifurcation curves in parameter space numerically for the case of an implicit selective predator, revealing the existence of a Hopf bifurcation.

Structured population models combine knowledge of individuals within the population (its basic unit) with notions of higher organisational levels. Their purpose is to describe the dependence of the dynamics of the whole population on the physiological state of the individuals, and vice versa, and are usually conceived as a frequency distribution of individuals which evolves over time. This aspect can be modelled by "structuring" the population with continuous, internal variables which represent a particular physiological feature. At the beginning of the last century, the most common variable used to model structured populations was age (see Abia et al. 2004

for a detailed description of such models and numerical methods employed to solve them). However, this variable has limited practical value due to the fact that age is very difficult to measure directly in a large number of species. As an alternative, other measurable physiological characteristics (such as length, mass, stage of maturity, energy reserves, amount of foliage, etc.; which can be grouped under the umbrella term "size") have been used to model the dynamics. Such studies led to the formulation of size-structured population models. We refer to Metz and Diekmann (1986) for a general exposition of the dynamics of size-structured populations and their theoretical framework.

Size-structured population models always involve at least one first-order hyperbolic partial differential equation for the distribution of the population over its "size"-domain, a nonlocal boundary condition which reflects the reproduction process, and an initial size-distribution for the population. The first theoretical results for size structured models were obtained by Ito et al. (1991) and demonstrated the existence and uniqueness of solutions for a linear model. The influence of total population size and temporal evolution was addressed in the work of Murphy (1983), where it was assumed that age, a, and size, x, were related and that, in a first stage, growth, g, depended only on size; Murphy wrote $x'(a) = g(x(a))$, known as "*Murphy's trick*," which permitted derivation of a size-structured model analogous to that of McKendrick–von Foerster. Murphy then introduced the idea that the vital functions depend explicitly on the total population, by means of the same technique. Before presenting the general system with an egg class in Sect. 2, we introduce a general model in which the vital functions depend explicitly both on time and a weighted average of the population (Angulo and López-Marcos 2004). Thus

$$u_t + \big(g\big(x, I_g(t), t\big)u\big)_x = -\mu\big(x, I_\mu(t), t\big)u, \quad 0 < x < 1,\ t > 0, \tag{1}$$

where $u(t, x)$ is the population density, and is a function both of time, t, and mass, x (normalised with respect to a maximum permitted size), and μ is the death rate. The nonlocal boundary condition (typically representing births) is given by

$$g\big(0, I_g(t), t\big)u(0, t) = \int_0^t \alpha\big(x, I_g(t), t\big)u(x, t)\,\mathrm{d}x, \quad t > 0, \tag{2}$$

for some kernel α, and the initial condition can be written

$$u(x, 0) = u_0(x), \quad 0 \le x \le 1. \tag{3}$$

Here, the functions $I_\mu(t)$, $I_\alpha(t)$ and $I_g(t)$ are defined as

$$I_\xi(t) = \int_0^1 \gamma_\xi(x)u(x, t)\,\mathrm{d}x, \quad t \ge 0, \tag{4}$$

where $\xi = \mu, \alpha$ and g. The scarce theoretical results related to nonlinear size-structured models are quite recent (for example, Tucker and Zimmerman 1988 and Calsina and Saldaña 1995). We refer to Abia et al. (2005) and the references therein for a wider review.

The increase of biological realism in these models is achieved at the expense of a significant loss of mathematical tractability; without simplifying assumptions, analytical solutions for models of this variety are difficult to obtain. Moreover, when

such models include additional nonlinearities and where the distinct physiological rates have environmental dependence, efficient numerical methods are the obvious and most suitable mathematical tools for studying the problem and, indeed, are often the only tools available. Nevertheless, the numerical approach to these equations has notable challenges that must be overcome owing to the nonlinear and nonlocal nature of the PDEs and boundary conditions. During the last two decades several numerical schemes have been proposed for solving age- and size-structured models. Here, we will give a brief outline of the most significant numerical methods documented in the literature for size dependent population models. We refer to Abia et al. (2004, 2005) and the references therein for a wider review, de Roos (1997) introduced the first numerical scheme in order to solve a similar model to (1–4), called the *escalator boxcar train*. Later, Ito et al. (1991) and Angulo and López-Marcos (1999) proposed numerical schemes (within a broad class of arbitrarily high order) for the linear problem based upon integration along the characteristic curves, employing the "*natural grid*." For a nonlinear model, where growth rate depends only on size, Angulo and López-Marcos (2000) introduced a second order method again utilising the natural grid along the characteristic curves to discretise an analytical representation of the solution. Kostova and Chipev (1991) developed a complete analysis for an explicit third order characteristics method, with the novelty that the total population functional $P(t)$ is approximated by discretising an ordinary differential equation that is satisfied by such a functional. Angulo and López-Marcos (2002) developed a full convergence analysis for a second order finite difference numerical method based on the box scheme for the solution of a nonlinear model where the growth rate depends also on time, in which they consider first the case of non-autonomous size-structured population models. Ackleh and Ito (1997) made the first attempt to solve the *fully nonlinear* model (1–4) (where $I_\alpha = I_\mu = I_g = 1$) by introducing an implicit finite difference method. Recently, Angulo and López-Marcos (2004) developed a full convergence analysis for second order numerical methods based on integration along characteristic curves with a moving mesh.

Numerical methods have been successfully applied to structured models to replicate available field and/or laboratory data, for a variety of different systems (e.g. demography, Angulo et al. 2010b, evolution of a forest, Zavala et al. 2007, cancer, Abia et al. 2010a, and different microorganisms, Abia et al. 2010b; Angulo et al. 2010a, 2011a, 2011b). For example, the effectiveness of the numerical scheme was demonstrated in Abia et al. (2009), Angulo et al. (2011c) for models of cell populations and Adimy et al. (2008) for a model of hematopoiesis. Solutions indicate that long-period oscillations can be obtained, corresponding to a destabilisation of the system. These oscillations can be related to observations of some periodic hematological diseases (such as chronic myelogenous leukemia).

For definiteness, we choose to study a recently proposed mass structured model for slug populations (Bees et al. 2006) with the aim of exploring solution behaviour in more detail using both analytical and numerical techniques. First, we must provide some background information.

Slugs cause much damage in agriculture and horticulture. Their economic impact is significant. The most popular means of control in an agricultural setting is the use of methiocarb or metaldehyde pellets. Unfortunately, these are thought to have

a deleterious effect on the environment including natural predators of slugs, such as the main predator, carabid beetles (Purvis and Bannon 1992). Organic farmers resort to a variety of control measures such as barriers or traps, but these are difficult to scale up. A promising modern approach is the use of the naturally occurring parasitic nematode *Phasmarhabditis hermaphrodita* (see the review by Rae et al. 2007, and references therein). However, there are major issues concerning cost-effective, efficacious deployment of this relatively expensive biocontrol. Optimal strategies are likely to combine detailed knowledge of slug dynamics as well as the behaviour and interactions of carabid beetles and nematodes.

It is clear from field studies that the dynamics of the slug *Deroceras reticulatum* (species dominant in the UK; a pest of global economic importance, South 1992) are highly irregular in stark contrast to the regular dynamics of less abundant species. Significant effort recently has been devoted to modelling populations of slugs (Shirley et al. 2001; Schley and Bees 2002, 2003; Choi et al. 2004, 2006; Bees et al. 2006) as well as slug biocontrol with nematodes (Wilson et al. 2004; Schley and Bees 2006). Generally, these models implicitly also include predation by carabid beetles. In Schley and Bees (2003, 2006) some attention was afforded to time delays at various tropic levels (e.g. slugs take on average nine months to mature to a stage where they are able to produce eggs). However, it was recognised that time delays were a somewhat artificial means of modelling these important aspects (Schley and Bees 2003, 2006). Furthermore, the mass of individual slugs varies enormously (two orders of magnitude) and carabid beetles are known to select their prey size carefully (Pollett and Desender 1986; Digweed 1993; Bohan et al. 2000; Symondson et al. 2002).

Examining field data, Hunter and Symmonds (1971) report unusual "leapfrogging" dynamics. They find that cohorts of slugs are interleaved; recently mature slugs give rise to eggs, and neither mature slugs nor eggs are directly related to an intermediate cohort of juveniles, which in turn are the offspring of a cohort of mature slugs of greater mass. However, the precise form of the mass distribution and whether cohorts overlap is unclear.

In order to explore these aspects further, Bees et al. (2006) developed a detailed mass structured model of slug dynamics with implicit predation by carabid beetles. Independent laboratory and field data were used extensively to construct tailored functional forms for the system. Although, simulations revealed a wealth of pulsed transient solutions, in the region of parameter space that was explored, asymptotic solutions were disappointingly dull. Therefore, the existence of pulse-like solutions appeared to rely on external influences. Here, we probe the model further for Hopf bifurcations and reveal that the dynamics allow for stable pulse solutions, which spontaneously arise in realistic regions of parameter space. Furthermore, in some regimes, leapfrogging populations are unavoidable.

We describe the model equations in the next section and present analytical results on solution existence, uniqueness and stability. In Sect. 3 we present the example system in more detail, namely a mass structured slug population model, and present explicit results from the analytical calculations described in the previous section and from a computational scheme. We go on to explore how boundary delays and selective predation affect the results. Finally, we conclude in Sect. 4, describing the implications for slug dynamics and future research directions.

2 Mass Structured System with an Egg Class

We shall start with the following age–mass structured system that explicitly includes an egg class for individuals, i.e. at a stage before they hatch with mass x_h. Hence, a balance of growth and death implies that

$$s_t^1(t,a) + s_a^1(t,a) = -\lambda_0 s^1(t,a), \tag{5}$$

and

$$s_t^2(t,x) + \big(\tilde{g}(x)s^2(t,x)\big)_x = -\tilde{\mu}\big(x, M(t)\big)s^2(t,x), \tag{6}$$

where $s^1(t,a)$ indicates the egg stage, and is a function of time, t, and age, $0 \le a \le a_h$, and $s^2(t,x)$ represents the adult stage and is a function of time and mass, $x_h \le x \le x_m$. Here, x_h represents the mass of recently hatched eggs of age a_h, and x_m indicates the maximum allowable mass of an adult individual (which may be infinite). The function $\tilde{g}(x)$ is the growth rate of adults, $\tilde{g}(x_m) = 0$, and λ_0 and $\tilde{\mu}^2(x, M(t))$ are the death rates, where $M(t)$ is a weighted population average to be discussed below. The initial conditions are

$$s^1(0,a) = s_0^1(a), \qquad s^2(0,x) = s_0^2(x), \tag{7}$$

and boundary conditions are given by

$$s^1(t,0) = \int_{x_h}^{x_m} \tilde{\beta}(x)s^2(t,x)\,\mathrm{d}x, \tag{8}$$

where $\tilde{\beta}(x)$ is the birth rate (egg production rate) of adults of mass x, and

$$\tilde{g}(x_h)s^2(t,x_h) = \int_0^{a_h} \delta(a-a_h)s^1(t,a)\,\mathrm{d}a \equiv s^1(t,a_h), \tag{9}$$

where $\delta(a)$ is the Dirac delta function.

Eggs generally have a negligible change in mass with time, but it is convenient to model both eggs and hatched individuals with the same variable x. Thus we define $x \ge x_h$ to represent mass and $x \le x_h$ to represent egg maturation stage. Such a representation also allows for seasonal effects on eggs to be included (Schley and Bees 2003; Bees et al. 2006). Thus we may combine the egg and adult stages by writing

$$s_t(t,x) + \big(g(x)s(t,x)\big)_x = -\mu\big(x, M(t)\big)s(t,x), \tag{10}$$

where s is the population density of eggs and adults,

$$s(t,x) := \begin{cases} \frac{a_h}{x_h}s^1\big(t, \frac{a_h}{x_h}x\big), & 0 \le x < x_h, \\ s^2(t,x), & x_h \le x \le x_m \end{cases}$$

and is a function both of size, x, and time, t. The initial conditions are

$$s(0,x) = s_0(x), \tag{11}$$

the boundary condition for the egg stage is given by

$$g(0)s(t,0) = \int_{x_h}^{x_m} \beta(x)s(t,x)\,\mathrm{d}x, \tag{12}$$

and the flux continuity condition for the hatching transition is

$$g\big(x_h^+\big)s\big(t,x_h^+\big)=g\big(x_h^-\big)s\big(t,x_h^-\big). \tag{13}$$

The function $g(x)$ is the combined growth rate and $\beta(x)$ the birth rate of individuals of mass x, and are given, respectively, in general form by

$$g(x)=\begin{cases}\frac{x_h}{a_h}, & 0\le x<x_h,\\ \tilde{g}(x), & x_h\le x\le x_m,\end{cases} \tag{14}$$

where a_h is the age at which the eggs hatch, and

$$\beta(x)=\begin{cases}0, & 0\le x<x_h,\\ \tilde{\beta}(x), & x_h\le x\le x_m.\end{cases} \tag{15}$$

Finally, the death rate is given by

$$\mu(x,M)=\begin{cases}\lambda_0, & 0\le x<x_h,\\ \tilde{\mu}(x,M), & x_h\le x\le x_m,\end{cases} \tag{16}$$

where

$$M(t)=\int_{x_h}^{x_m} m(x)s(t,x)\,\mathrm{d}x, \tag{17}$$

and $m(x)$ is an appropriate kernel. For example, $M(t)$ might be the total biomass and then $m(x)=x$.

It is possible to convert such a system to one of age structure rather than of mass, but here we preserve the mass structure as (a) the functional forms are readily interpreted, (b) mass data are more readily available for the applications that we have in mind, and (c) non-autonomous extensions to our example system require a time dependent growth rate that cannot practicably be modelled by a system with age structure.

We shall further develop this equation in later sections to include predation, but for now shall adopt the above predation-free structure. The egg stage takes on a particularly simple form that allows for immediate integration to yield

$$s(t,x)=\frac{a_h}{x_h}B(t,x)\exp\left(-\lambda_0 a_h\frac{x}{x_h}\right), \tag{18}$$

where $B(t,x)=g(0)s(t-a_h\frac{x}{x_h},0)$ (which can be expanded as in Eq. (12)). Thus we obtain the delay system

$$\begin{cases}s_t(t,x)+\big(g(x)s(t,x)\big)_x=-\mu\big(x,M(t)\big)s(t,x), & x_h\le x\le x_m,\\ g(x_h)s(t,x_h)=e^{-\lambda_0 a_h}\displaystyle\int_{x_l}^{x_m}\beta(x)s(t-a_h,x)\,\mathrm{d}x,\\ s(t,x)\quad\text{is known for } -a_h\le t\le 0.\end{cases} \tag{19}$$

Here, x_l, where $x_h<x_l<x_m$, represents the maturation slug size; i.e. the lower bound of the support of the birth rate.

2.1 Existence of Non-Trivial Steady States

The trivial steady state, $s \equiv 0$, always satisfies the system (19). Now consider that there exists a non-trivial solution $s = u(x)$ that is independent of time. Then

$$\begin{aligned} \big(g(x)u(x)\big)_x &= -\mu\big(x, M^*\big)u(x), \\ g(x_h)u(x_h) &= \exp(-\lambda_0 a_h)\int_{x_l}^{x_m} \beta(x)u(x)\,\mathrm{d}x, \end{aligned} \tag{20}$$

where $M^* = \int_{x_h}^{x_m} m(x)u(x)\,\mathrm{d}x$. Using the notation $B^* = \int_{x_l}^{x_m} \beta(x)u(x)\,\mathrm{d}x$, then

$$\begin{aligned} g(x)u(x) &= g(x_h)u(x_h)\exp\bigg(-\int_{x_h}^{x} \frac{\mu(\sigma, M^*)}{g(\sigma)}\,\mathrm{d}\sigma\bigg) \\ &= B^*\exp(-\lambda_0 a_h)\exp\bigg(-\int_{x_h}^{x} \frac{\mu(\sigma, M^*)}{g(\sigma)}\,\mathrm{d}\sigma\bigg), \end{aligned} \tag{21}$$

and so

$$u(x) = B^*\exp(-\lambda_0 a_h)S^*\big(x, M^*\big), \tag{22}$$

where

$$S^*\big(x, M^*\big) = \frac{1}{g(x)}\exp\bigg(-\int_{x_h}^{x} \frac{\mu(\sigma, M^*)}{g(\sigma)}\,\mathrm{d}\sigma\bigg). \tag{23}$$

Therefore, we find that the steady-state solution, $u(x)$, satisfies the nonlinear expression

$$u(x) = \exp(-\lambda_0 a_h)\bigg(\int_{x_l}^{x_m} \beta(x)u(x)\,\mathrm{d}x\bigg)S^*\big(x, M^*\big). \tag{24}$$

Thus this condition implies that

$$B^* = B^*\exp(-\lambda_0 a_h)\int_{x_l}^{x_m} \beta(x)S^*\big(x, M^*\big)\,\mathrm{d}x, \tag{25}$$

which, hence, provides the transcendental equation

$$1 = \exp(-\lambda_0 a_h)\int_{x_l}^{x_m} \beta(x)S^*\big(x, M^*\big)\,\mathrm{d}x, \tag{26}$$

which can be rewritten as

$$1 = \exp(-\lambda_0 a_h)\int_{x_l}^{x_m} \frac{\beta(x)}{g(x)}\exp\bigg(-\int_{x_h}^{x} \frac{\mu(\sigma, M^*)}{g(\sigma)}\,\mathrm{d}\sigma\bigg)\,\mathrm{d}x. \tag{27}$$

If we define $H(\Phi) = \exp(-\lambda_0 a_h)\int_{x_l}^{x_m} \beta(x)S^*(x, \Phi)\,\mathrm{d}x$, then a non trivial steady state must satisfy $H(M^*) = 1$.

Theorem 1 (Existence of Non-Trivial Equilibria) *Let $\mu(x, \Phi)$ be an increasing function with respect to the second variable. The condition $H(0) > 1$ is necessary and sufficient for a non-trivial steady state to exist, and it is unique.*

Proof We know that $\mu(x,\Phi)$ is an increasing function on the variable Φ, then $H(\Phi)$ is decreasing on Φ. Also, we know that $\lim_{\Phi\to\infty} H(\Phi)=0$. Therefore, if $H(0)>1$ then we have a unique non-trivial steady state. Otherwise, only the trivial steady state appears. □

An estimate for M^* can be established from the nonlinear Eq. (27) by applying an iterative scheme (e.g. Newton–Raphson, bisection, etc.). Then we may compute B^* by means of

$$M^*=\int_{x_h}^{x_m} m(x)u(x)\,\mathrm{d}x = B^*\exp(-\lambda_0 a_h)\int_{x_h}^{x_m} m(x)S^*\big(x,M^*\big)\,\mathrm{d}x,$$

which implies

$$B^*=\frac{M^*\exp(\lambda_0 a_h)}{\int_{x_h}^{x_m} m(x)S^*(x,M^*)\,\mathrm{d}x}. \tag{28}$$

The solution follows from Eqs. (22) and (23).

2.2 Linearisation Around the Nontrivial Steady State

In this section, we linearise in a neighbourhood of the equilibrium point by setting $s(x,t)=u(x)+\varepsilon(x,t)$, where $\varepsilon(x,t)\ll 1$. Then, by definition, $M(t)=M^*+\bar{M}(t)$, where $\bar{M}(t)=\int_{x_h}^{x_m} m(x)\varepsilon(x,t)\,\mathrm{d}x$, and $\varepsilon(x,t)$ satisfies

$$\begin{aligned}\varepsilon_t+\big(g(x)\varepsilon\big)_x &= -\bar{M}(t)\mu_M\big(x,M^*\big)B^*\exp(-\lambda_0 a_h)S^*\big(x,M^*\big)\\ &\quad-\mu\big(x,M^*\big)\varepsilon(x,t),\end{aligned} \tag{29}$$

with boundary condition

$$g(x_h)\varepsilon(x_h,t)=\exp(-\lambda_0 a_h)\int_{x_l}^{x_m}\beta(x)\varepsilon(x,t-a_h)\,\mathrm{d}x, \tag{30}$$

where μ_M refers to a derivative with respect to the second argument. The integrable continuous solutions with separate variables of the linearised system are given by $\varepsilon(x,t)=\varepsilon(x)e^{\gamma t}$, where $\gamma\in\mathbb{C}$ (eigenvalue) is a constant. The function $\varepsilon(x)$ satisfies

$$\begin{aligned}\big(g(x)\varepsilon(x)\big)' &= -\nu\mu_M\big(x,M^*\big)B^*\exp(-\lambda_0 a_h)S^*\big(x,M^*\big)\\ &\quad-\big(\mu\big(x,M^*\big)+\gamma\big)\varepsilon(x),\end{aligned} \tag{31}$$

with boundary condition

$$g(x_h)\varepsilon(x_h)=\exp\big(-(\lambda_0+\gamma)a_h\big)\int_{x_l}^{x_m}\beta(x)\varepsilon(x)\,\mathrm{d}x, \tag{32}$$

where $\bar{M}(t)=e^{\gamma t}\nu$, and $\nu=\int_{x_h}^{x_m} m(x)\varepsilon(x)\,\mathrm{d}x$.

From Eq. (31) we have

$$\begin{aligned}&\left(\exp\left(\int_{x_h}^{x}\frac{\mu(\sigma,M^*)+\gamma}{g(\sigma)}\,\mathrm{d}\sigma\right)g(x)\varepsilon(x)\right)'\\ &\quad=-\nu\mu_M\big(x,M^*\big)B^*e^{(-\lambda_0 a_h)}S^*\big(x,M^*\big)\exp\left(\int_{x_h}^{x}\frac{\mu(\sigma,M^*)+\gamma}{g(\sigma)}\,\mathrm{d}\sigma\right),\end{aligned} \tag{33}$$

and if we set

$$G(x) = \exp\left(\int_{x_h}^{x} \frac{1}{g(\sigma)}\,\mathrm{d}\sigma\right), \tag{34}$$

then

$$\left(G(x)^{\gamma}\frac{\varepsilon(x)}{S^*(x,M^*)}\right)' = -\nu\mu_M\big(x,M^*\big)B^*\exp(-\lambda_0 a_h)\frac{1}{g(x)}G(x)^{\gamma}. \tag{35}$$

Integration between x_h and x yields

$$G(x)^{\gamma}\frac{\varepsilon(x)}{S^*(x,M^*)} - \varepsilon(x_h)g(x_h) = -\nu\mu_M\big(x,M^*\big)B^*\exp(-\lambda_0 a_h)\int_{x_h}^{x}\frac{G(\sigma)^{\gamma}}{g(\sigma)}\,\mathrm{d}\sigma. \tag{36}$$

Setting

$$F_{\gamma}(x) = \mu_M\big(x,M^*\big)\int_{x_h}^{x}\frac{G(\sigma)^{\gamma}}{g(\sigma)}\,\mathrm{d}\sigma = \frac{\mu_M(x,M^*)}{\gamma}\big[G(x)^{\gamma}-1\big], \tag{37}$$

we arrive at

$$\varepsilon(x) = \frac{S^*(x,M^*)}{G(x)^{\gamma}}\big(\varepsilon(x_h)g(x_h) - \nu B^*\exp(-\lambda_0 a_h)F_{\gamma}(x)\big). \tag{38}$$

Here, note that whilst the values of $g(x_h)$, λ_0, a_h, M^* and B^*, and the functions $S^*(x,M^*)$, and $G(x)$ can be estimated, the values of γ, $\varepsilon(x_h)$ and μ have yet to be determined ($F_{\gamma}(x)$ can be computed once a value of γ has been obtained).

To compute ν we substitute Eq. (38) into the definition $\nu = \int_{x_h}^{x_m} m(x)\varepsilon(x)\,\mathrm{d}x$ and rearrange to give

$$\nu = \frac{\varepsilon(x_h)g(x_h)\int_{x_h}^{x_m} m(x)\frac{S^*(x,M^*)}{G(x)^{\gamma}}\,\mathrm{d}x}{1 + B^*\exp(-\lambda_0 a_h)\int_{x_h}^{x_m} m(x)\frac{S^*(x,M^*)}{G(x)^{\gamma}}F_{\gamma}(x)\,\mathrm{d}x}. \tag{39}$$

Therefore, substitution of ν back into Eq. (38) provides

$$\varepsilon(x) = \frac{S^*(x,M^*)}{G(x)^{\gamma}}\varepsilon(x_h)g(x_h)\big(1 - f_{\gamma}F_{\gamma}(x)\big) \tag{40}$$

where

$$f_{\gamma} = \frac{B^*\exp(-\lambda_0 a_h)\int_{x_h}^{x_m} m(x)\frac{S^*(x,M^*)}{G(x)^{\gamma}}\,\mathrm{d}x}{1 + B^*\exp(-\lambda_0 a_h)\int_{x_h}^{x_m} m(x)\frac{S^*(x,M^*)}{G(x)^{\gamma}}F_{\gamma}(x)\,\mathrm{d}x}. \tag{41}$$

Finally, applying boundary condition (32) gives

$$g(x_h)\varepsilon(x_h) = e^{(-(\lambda_0+\gamma)a_h)}\int_{x_l}^{x_m}\beta(x)\frac{S^*(x,M^*)}{G(x)^{\gamma}}\varepsilon(x_h)g(x_h)\big(1 - f_{\gamma}F_{\gamma}(x)\big)\,\mathrm{d}x, \tag{42}$$

and thus the parameter γ must satisfy the characteristic equation

$$1 = \exp\big(-a_h(\lambda_0+\gamma)\big)\int_{x_l}^{x_m}\beta(x)\frac{S^*(x,M^*)}{G(x)^{\gamma}}\big(1 - f_{\gamma}F_{\gamma}(x)\big)\,\mathrm{d}x. \tag{43}$$

In principle, this equation can be solved for the perturbation growth rate γ given the existence of the steady state (and the starred quantities) and all of the parameter values. In practice, the problem is terribly complex and numerical solutions are extremely difficult to obtain. So, instead, we restrict attention to a full numerical treatment of the problem. However, in Appendix A we sketch the method for the special case of a Hopf bifurcation. In order to proceed numerically we must specify the precise form of each function. Therefore, in the next section we describe a particular application of the theory in order to obtain explicit results.

3 Application to Slug Population Dynamics

Here, we present the nonlinear, size-structured model for slug dynamics including an egg class (boundary delay) as well as selective predation by carabid beetles as described by Bees et al. (2006). We refer the interested reader to Bees et al. (2006) for an unabridged description of the model and a comprehensive account of the functional forms. The parameters are determined from laboratory and field data and are tabulated in Table 1 for convenience. The model is as stated in Eq. (19), with growth rate, death rate and birth kernel defined, respectively, as

$$g(x) = \begin{cases} \frac{x_h}{a_h}, & 0 \le x < x_h, \\ \frac{(x-x_m)^2}{g_2}, & x_h \le x \le x_m, \end{cases}$$

Table 1 Parameter values for numerical simulations of the model as tabulated in Bees et al. (2006). Here † indicates values obtained by fitting appropriate functional forms to data

Symbol	Description (with references)	Standard model	Other values
a_h	Mean egg hatching time (Hunter and Symmonds 1971)	70 d	
x_h	Size of newly hatched slugs (South 1992)	10.0 mg	
x_l	Maturation slug size (South 1982)	425 mg	
x_m	Max slug size (South 1982) ($\equiv g_1$) †	922 mg	
x_p	Preferred prey size (Digweed 1993)	40.0 mg	100; 450
x_w	Half prey distribution width	10.0 mg	30; 90
x_e	Slug size of peak egg production (South 1982) †	445 mg	500
p_h	Level of half max predation	0 mg	$(0.1; 0.5; 0.9) \times p_m$
p_m	Max predation rate	0 mg d^{-1}	$(\frac{1}{10}; 1; 3) \times \Pi_{\max}$
$\Pi_{\max}$	Max predation target	$\max_t \Pi(t)$	
ϖ	Egg production cost	0 d^{-1}	0.00145
K_0	Environmental carrying capacity (Schley and Bees 2003) †	2.68×10^8 mg d	2.68×10^6 or 10^{10}
g_2	Growth constant (South 1982) †	1.41×10^5 mg^{-1} d	
β_1	Max egg production rate (Carrick 1938)	1.40 $\frac{\text{eggs}}{\text{slug}}\mathrm{d}^{-1}$	
λ_0	Egg death rate (South 1992) †	1.52×10^{-2} d^{-1}	
λ_1	Intrinsic slug death rate (South 1982, 1992; Choi et al. 2004) †	1.45×10^{-3} d^{-1}	0.0254; 1.45×10^{-4}

$$\mu(x, M, \Pi) = \begin{cases} \lambda_0, & 0 \le x < x_h, \\ \lambda_1 + \lambda_2 x^{\lambda_3} + \frac{M}{K_0} + f(x)\frac{p_m \Pi^2}{p_h^2 + \Pi^2} + \varpi\beta(x), & x_h \le x \le x_m, \end{cases}$$

and

$$\beta(x) = \begin{cases} 0, & 0 \le x < x_l, \\ \beta_1 \hat{\beta}(x), & x_l \le x \le x_m, \end{cases}$$

where

$$\hat{\beta}(x) = \frac{x - x_l}{x_e - x_l} \exp\left(1 - \frac{x - x_l}{x_e - x_l}\right). \tag{44}$$

Here g_2 is a growth constant, λ_1, λ_2 and λ_3 are slug death parameters, x_p, p_m and p_h are selective predation parameters, ϖ is the egg production cost, x_e is the slug size at peak egg production ($x_l \le x_e$) and

$$\Pi(t) = \int_{x_h}^{x_m} x f(x) s(t, x)\, \mathrm{d}x,$$

represents the "slug target" to size selective predators (carabid beetles), where

$$f(x) = \begin{cases} \frac{1}{x_w}(\cos(\frac{\pi(x - x_p)}{2x_w}))^2, & |x - x_p| < x_w, \\ 0, & \text{otherwise}, \end{cases}$$

is the slug size weighting function. Furthermore,

$$M(t) = \int_{x_h}^{x_m} x s(t, x)\, \mathrm{d}x,$$

(so that $m(x) = x$) as well as the slug carrying capacity, K_0, are considered to be in units of the total slug biomass. As stated above, all of the parameters are measured or estimated from laboratory or field data and, together with the functional forms, are discussed in detail in Bees et al. (2006).

The death rate μ takes a form that is more general than that considered in the previous section but, apart from the predation term (i.e. the term multiplied by p_m) the extra terms were found in Bees et al. (2006) not to play a significant role. Therefore, for the sake of clarity (the results can be generalised in a straightforward manner) we shall assume that $\lambda_2 = \varpi = 0$. As the egg stage has been incorporated as a boundary delay then $x_h \le x_l \le x \le x_m$. For the analytical studies we shall restrict attention to $p_m = 0$, but shall consider $p_m \ge 0$ for the numerical exploration. In such cases, $x_p \in [x_h + x_w, x_m - x_w]$.

3.1 Non-Trivial Steady State

One of the purposes of the analytical work in this section is to support the numerical computations by demonstrating that solutions are real and not a consequence of the numerical method. This is practicable for the nontrivial solution existence criterion. With this in mind we simplify the equations slightly in this section by setting $p_m = 0$.

With the above function definitions, the equation to determine the non-trivial steady solution is as in Eq. (27). We may solve this equation for M^* as a function

of the control parameter β_1. The birthrate parameter β_1 is a suitable choice of control parameter as (A) it significantly affects the dynamics, (B) it is dependent on environmental conditions, and (C) it may serve as a target for pest control measures. A solution to this equation can be obtained from a Newton–Raphson or bisection approach, or similar. Alternatively, using the parameter values as in Table 1 (except for β_1) and Eq. (27), non-trivial solutions exist if and only if $M^* > 0$, which is true if and only if

$$\beta_1 > \frac{\exp(\lambda_0 a_h)}{\int_{x_l}^{x_m} \frac{\hat{\beta}(x)}{g(x)} \exp(-\int_{x_h}^{x} \frac{\mu(\sigma,0)}{g(\sigma)}\,\mathrm{d}\sigma)\,\mathrm{d}x}, \tag{45}$$

which in turn provides the criterion $\beta_1 > 0.097968$ (5 s.f.). We shall return to this value shortly.

3.2 Numerical Exploration of Parameter Space

In this section, we present a numerical scheme to simulate the full system, and demonstrate that we have agreement with analytical calculations, lending credence to the qualitative and quantitative validity of the numerical results. The numerical algorithm is similar to that employed in Bees et al. (2006) and is summarised in Appendix B.

The range of β_1, the maximum egg production rate per day, deserves some discussion. The value chosen for simulations (Bees et al. 2006) of $\beta_1 = 1.4$ eggs slugs^{-1} d^{-1} was derived from field data with a functional form based on size from laboratory data (South 1982, 1992; Bees et al. 2006) (a smoothly attained peak after maturity followed by a gradual decline in egg production rate per slug with age). Bees et al. (2006) restricted attention to simulations with a fixed value of β_1. However, it is clear that there is scope for variation of this parameter, certainly within an order of magnitude. We find that the qualitative dynamics are sensitive to β_1 in a manner unlike other parameters (explored in Bees et al. 2006), and thus we choose it as a bifurcation parameter.

For sufficiently small values of β_1 (over the range of realistic values for the other parameters) the numerical method reveals that all initial conditions decay to zero. At some critical value a bifurcation results in a non-trivial solution. For the selected parameter values this occurs at $\beta_1 = 0.098$, agreeing with the theoretical calculation in Sect. 3.1.

In Fig. 1, plotting total biomass with time, we present four distinct solution behaviours for a typical, fixed, non-zero value of the predation rate $p_m = 0.1$. In each panel, after the initial decay of a large peak, associated with the collapse of transients onto an attractor, a range of behaviours are observed over many days. The traits of the solutions are illustrated better in Fig. 2 where we plot total biomass against total population for the same parameters as in Fig. 1. In both figures, panel (a) exhibits the decay of transients to an equilibrium solution for $\beta_1 = 1$. Plotting the mass distribution yields an equilibrium solution similar to those investigated in Bees et al. (2006).

For $\beta_1 = 2.6$, panel (b) displays a solution where transients decay to a limit cycle. For this parameter value, we plot the population density as a function of mass and

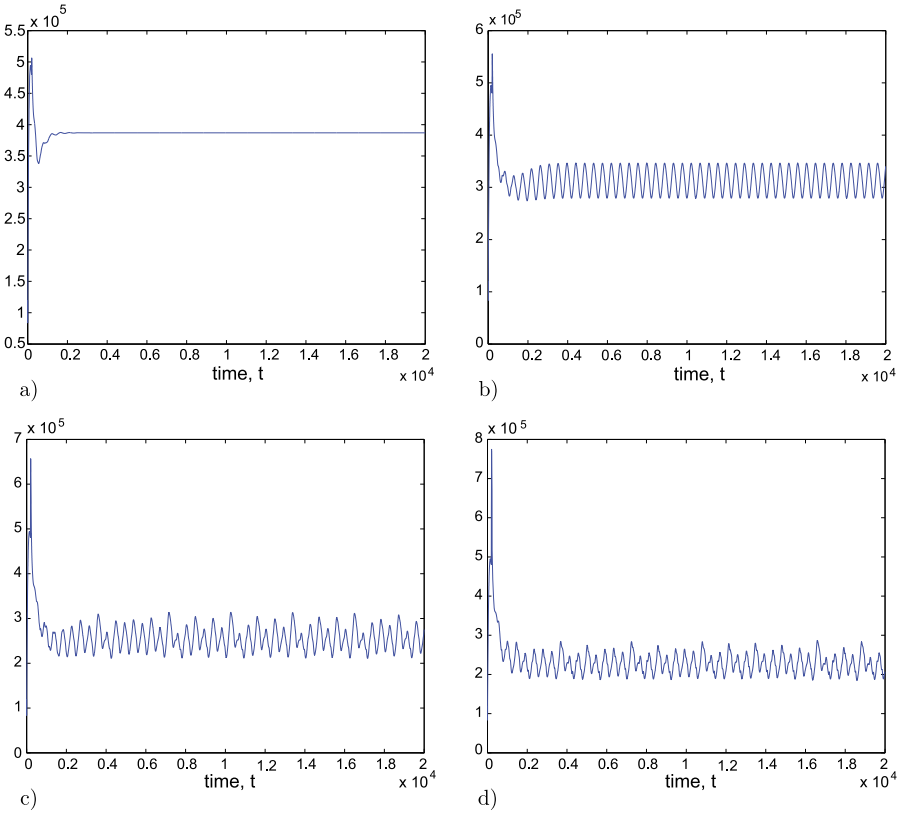

Fig. 1 Plots of total biomass with time for fixed $p_m = 0.1$. (**a**) $\beta_1 = 1$, decay of transients to equilibrium, (**b**) $\beta_1 = 2.6$, oscillations, (**c**) $\beta_1 = 6$, solutions slowly approach a period two oscillation, and (**d**) $\beta_1 = 10$, apparent chaos (Colour figure online)

time in Fig. 3 and the contours of the biomass in Fig. 4. It is clear that distinct pulse solutions exist that give rise to the oscillations in total population and biomass in Figs. 1 and 2. These pulse solutions have a characteristic shape with an initially rapid increase in mass which slows as individuals mature.

There is a sudden transition between the behaviour in panels (a) and (b) of Figs. 1 and 2, a Hopf bifurcation. In Figs. 5 and 6 we plot two Hopf bifurcation diagrams obtained from brute force, long-time numerical calculations, each as a function of two control parameters: in Fig. 5, β_1 and p_m (the maximum predation rate) are varied; in Fig. 6, β_1 and a_h (the time taken for eggs to hatch) are varied. For small values of p_m the stable pulse solutions are rather weak (i.e. considerable overlap between cohorts) and require a large value of β_1 to exist. The solutions appear to be closer to simple oscillations about the equilibrium solution. As p_m is increased to a value of approximately 0.1, the oscillations gain a pulse aspect, as observed in Fig. 4, and require a relatively small value of β_1. Beyond $p_m = 0.1$, the stable, well-defined pulse solutions require a larger and larger value of β_1 to exist. These solutions have diminished amplitude due to the harsh predatory response. Fixing $p_m = 0.1$ we find in Fig. 6

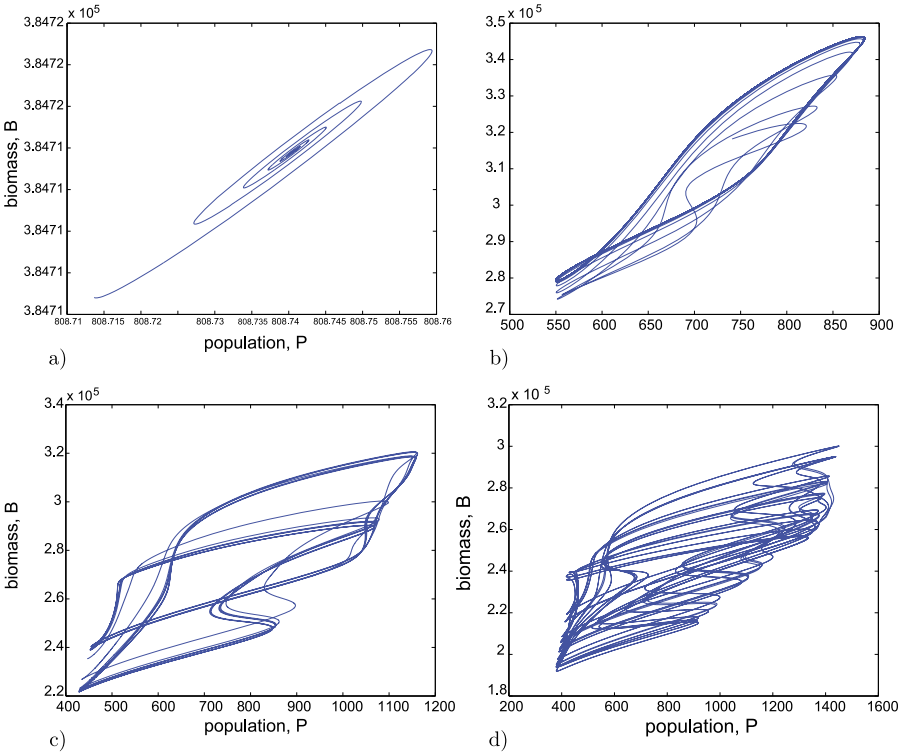

Fig. 2 A plot of total biomass with total population for fixed $p_m = 0.1$ and various values of β. Four subplots with (**a**) $\beta_1 = 1$, (**b**) $\beta_1 = 2.6$, (**c**) $\beta_1 = 6$, and (**d**) $\beta_1 = 10$, illustrating equilibrium, limit cycle, period doubling and apparent chaos, respectively (Colour figure online)

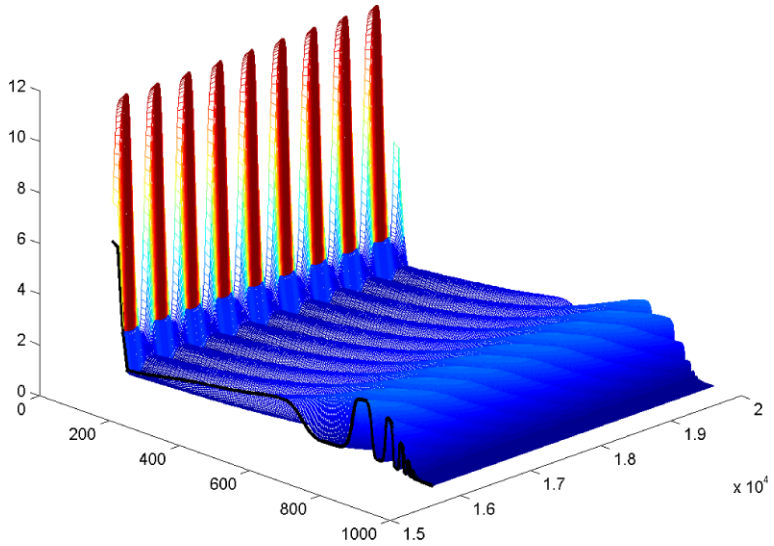

Fig. 3 Evolution of population density structure with time for $p_m = 0.1$ and $\beta = 2.6$. Large peaks of slugs with low mass evolve to stable pulse solutions. Time is measured in days (d) (Colour figure online)

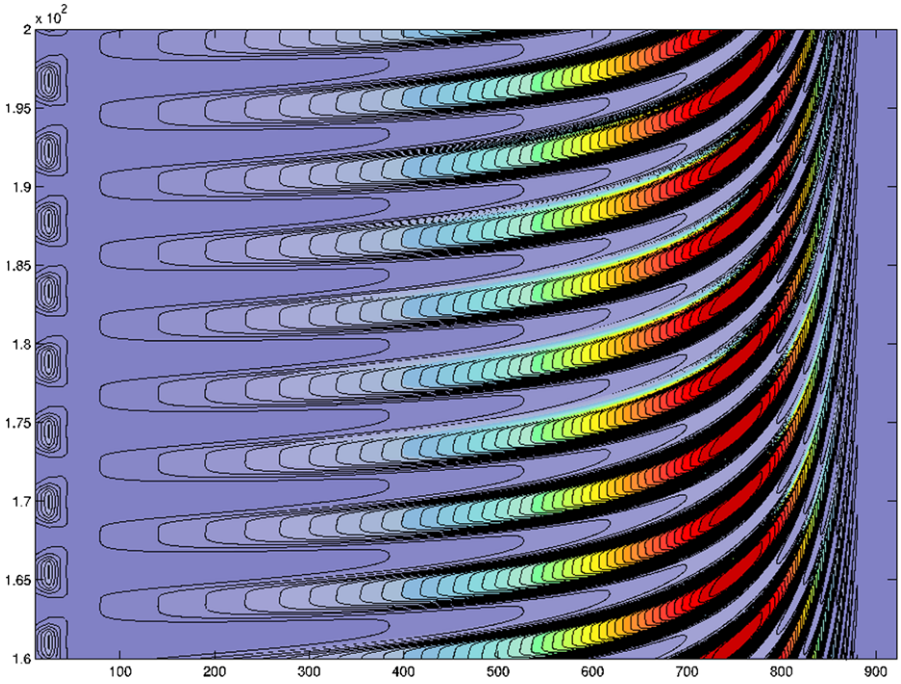

Fig. 4 Example of mass density structure with time for $p_m = 0.1$ and $\beta = 2.6$. The pulsed solutions are clearly defined, although with some overlap (see text) (Colour figure online)

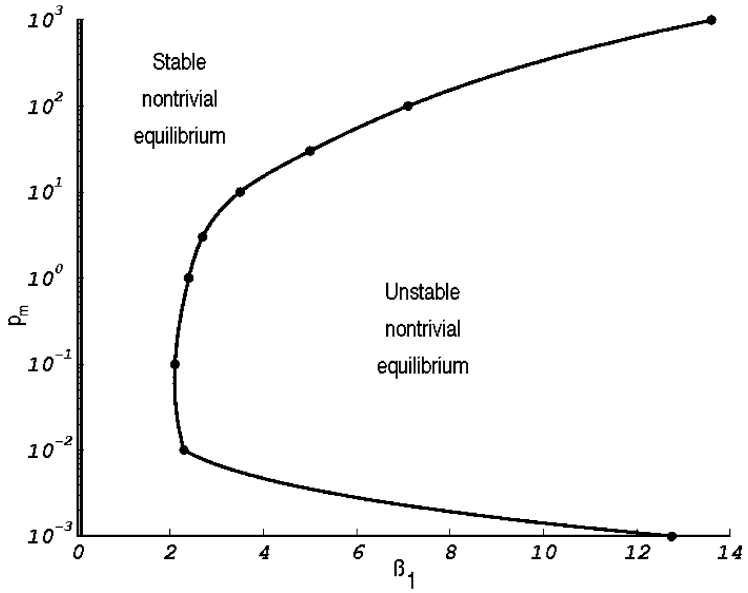

Fig. 5 Bifurcation diagram (β_1 and p_m space): analytical (*straight vertical line*; for non-trivial steady-state existence) and numerical results (*filled circles*; Hopf bifurcation)

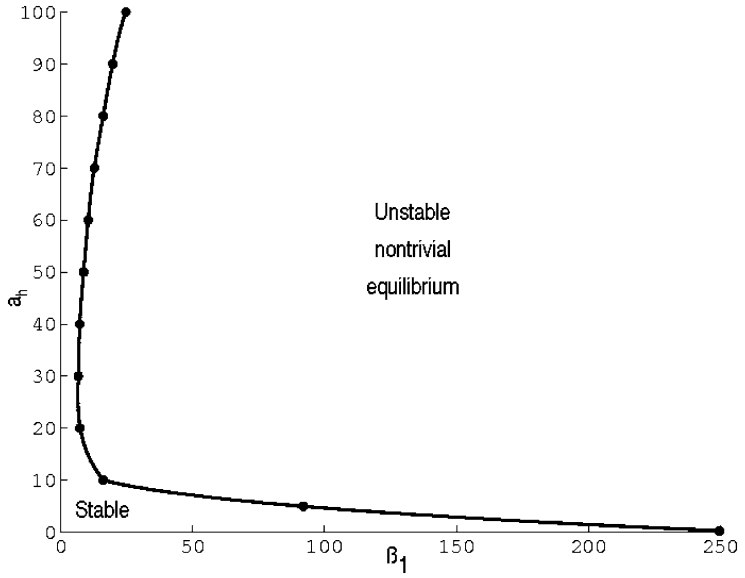

Fig. 6 Bifurcation diagram (β_1 and a_h space) for the impact of the boundary delay, a_h, where $p_m = 0.1$. The *curve* represents a Hopf bifurcation, resulting from the destabilisation of the non-trivial equilibrium solution

that we get a similar bifurcation curve as we vary a_h. However, the mechanisms are different. The normal value of the mean time it takes for a slug egg to hatch is approximately 70 days. This is a fairly well established value (Hunter and Symmonds 1971). However, we may vary this value to assess the impact of a boundary delay. Increasing a_h increases the required value of β_1 for oscillations. The minimum occurs between $a_h = 20$ and 30, and smaller values of a_h rapidly increase the required value of β_1 for oscillations. Pulse solutions are still possible for $a_h = 0$, but we also must have $\beta_1 > 250$, which is somewhat unrealistically large. (Note that setting both $p_m = 0$ and $a_h = 0$ does not appear to admit a stable oscillatory solution.) It is perhaps intuitive that an intermediate value of the egg mean hatching time, a_h, should facilitate pulsed solutions.

In Figs. 1(c) and 2(c) for $\beta_1 = 6$, we find a solution that appears to tend towards a period 2 limit cycle. However, the precise form of the limit cycle is by no means clear, and does not improve significantly over longer simulation runs. If the solution is a genuine period two oscillation then the variations about it may be due to very long transients or numerical artifacts. We have observed similar behaviour for a range of other parameters, but the boundary between solutions in panels (b) and (c) is not clear. Furthermore, period four, and others, are irregularly discernable for slightly larger values of β.

Increasing β_1 further to a value of 10, yields chaotic-like solution behaviour, as can be observed in Figs. 1(d) and particularly in 2(d). There is a clear departure from the fairly regular dynamics in panels (c) to the very unpredictable dynamics in panels (d).

Leapfrogging behaviour is also apparent for larger values of β (see Fig. 7). Pulses emerge that are sufficiently widely spaced to allow/encourage the development of

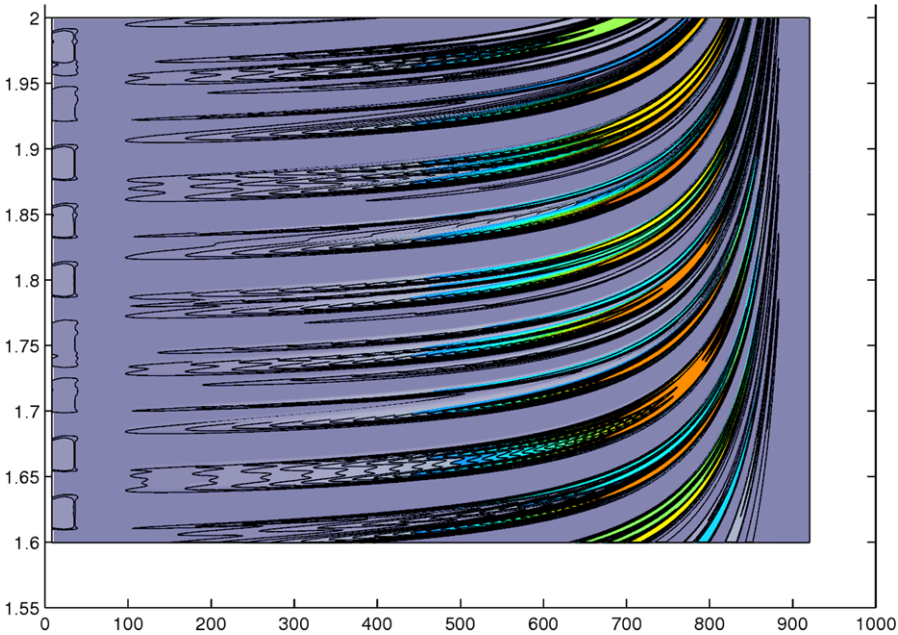

Fig. 7 Example of mass density structure with time for $p_m = 0.1$ and $\beta = 10$. The pulsed solutions are clearly defined, with a leapfrogging signature (see text) (Colour figure online)

interleaved non-related cohorts. In other words, newly mature adults lay eggs and are not directly related to intermediate cohorts of juveniles and a cohort of immediately older mature adults. They may, however, be descendents of much older adults. Such behaviour has been observed in field data (Hunter and Symmonds 1971). However, it must be stated that there is a degree of overlap between cohorts, although of course the overlap is stable, in the sense that the equally spaced pulse solutions are approached asymptotically. These chaotic-like leapfrogging solution appears to be globally stable; other initial conditions lead eventually to the leapfrogging solution.

It must be remembered that the governing equations are such that the cohorts are all coupled through nonlinear and nonlocal terms. Not least, the action of selective predation, which plays a key role in separating cohorts (see discussion below).

4 Conclusions

In this paper, we introduce a general class of mass structured system with a boundary delay due to an egg class. We investigate the existence and uniqueness of nontrivial solutions, and explore the analysis of stability. In particular, we derive criteria for the existence of a nontrivial solution and for a Hopf bifurcation. Then, we apply these analyses to an example model of slug dynamics. We find that we can determine the existence and uniqueness of non-trivial steady states, but are unable to progress work on stability owing to the excessive complications and thus cumbersome numerical approximations required to compute additional bifurcation points. Instead, we pursue

a full numerical treatment of the nonlinear and nonlocal mass structured system with a boundary delay and selective predation. We adapt a recent method, with integration along characteristics employing a moving grid, for this purpose. Good agreement was obtained between numerical calculations and the (limited) analytical results obtained.

Novel pulse solutions are found to exist for a range of parameter values. Using the egg production rate, β_1, as the main bifurcation parameter, we find that there are transitions from trivial equilibrium solutions for small β_1, through a bifurcation to nontrivial equilibrium solutions, followed by a Hopf bifurcation with general oscillations or pulsed solutions (depending on selective predation), with what appears to be a weakly defined period doubling cascade to chaotic-like solutions of various mixed pulses. In rough terms, the boundary delay (egg stage) appears to allow for generally oscillating solutions whereas selective predation tends to admit pulses. However, only weak oscillations are possible with small values of the mean egg hatching time, a_h, or levels of predation, p_h, and these require an unrealistically large value of β_1. This is also true if a_h or p_h are too large. The most unstable situation (i.e. most accommodating to oscillations/pulses) occurs when there is an intermediate combination of boundary delay and selective predation, well within the range of realistic parameter values. To obtain oscillations, the combination requires a value of β_1 a factor of six smaller than for selective predation alone, and two orders of magnitude smaller than for boundary delay alone.

One effect of the selective predation term is to preferentially bias short pulses (cohorts). In other words, as individuals gain mass and a pulse of such individuals travels through the target mass zone of the predators, the predators respond by increasing predation. Pulses wider than the predation zone are predated more in the centre of the pulse, which when combined with nonlocal terms can lead to pulse separation. The boundary delay induces a separate instability mechanism based upon time out from the feedback dynamics.

The novel chaotic-like dynamics discussed above display leapfrogging behaviour (i.e. interleaved generations) as observed in field data (Hunter and Symmonds 1971) back in 1971. This is the first time that such dynamics have been observed in models, certainly for slugs and, to the best of our knowledge, for any other species. We hypothesise that the mechanism is due to the combined effects of selective predation and a boundary delay, allowing and enhancing intermediate cohorts.

In summary, boundary delays and selective predation can induce oscillatory and pulse solutions, and there are parameter regimes where leapfrogging solutions are dominant. There are, however, other candidates for generating pulse solutions, and these need to be investigated in detail. More involved dynamics, such as explicit predator-prey interactions, may be easily implemented and will likely generate oscillations. The same is true of implementing spatial aspects and temporal (i.e. seasonal) forcing. However, due to a lack of experimental data on carabid beetles and other predators, the precise forms of the governing equations are not clear. In order to avoid biasing models towards oscillating systems a rigorous approach must be adhered to, led by experimental fact. Such data are recently becoming available (e.g. see Bohan et al. 2000; Symondson et al. 2002), so advances in these directions should be possible.

Acknowledgements The authors are grateful to both anonymous referees for their valuable help to improve the manuscript. The authors would like to thank D. Schley for useful discussions. O.A. and J.C.L. are supported in part by the grants from the Ministerio de Ciencia e Innovación (Spain), MTM2011-25238, the Junta de Castilla y León and Unión Europea F.S.E. VA046A07, and by the 2009 Grant Program for Excellence Research Group (GR137) of the Junta de Castilla y León. M.A.B. is supported by EPSRC EP/D073308/1.

Appendix A: Hopf Bifurcation

Following on from Eq. (43), for a Hopf bifurcation, we put $\gamma = \mathrm{i}\alpha$, where $\alpha \in \mathbb{R}$. For convenience, set

$$h(x) = \int_{x_h}^{x} \frac{1}{g(\sigma)}\,\mathrm{d}\sigma, \tag{46}$$

so that $G(x) = \exp(h(x))$. Then

$$G^{\gamma}(x) = G^{\mathrm{i}\alpha}(x) = \cos\big(\alpha h(x)\big) + \mathrm{i}\sin\big(\alpha h(x)\big), \tag{47}$$

and

$$\begin{aligned} F_{\gamma}(x) &= \frac{\mu_M(x, M^*)}{\gamma}\big[G(x)^{\gamma} - 1\big] \\ &= \frac{1}{K\alpha}\big[\sin\big(\alpha h(x)\big) + \mathrm{i}\big(1 - \cos\big(\alpha h(x)\big)\big)\big], \end{aligned} \tag{48}$$

where we define

$$K\big(x, M^*\big) = 1/\mu_M\big(x, M^*\big) \tag{49}$$

for notational convenience (see definition of carrying capacity in Sect. 3). Also we find that

$$\begin{aligned} &f_{\gamma} \\ &= \frac{B^* e^{(-\lambda_0 a_h)} \int_{x_h}^{x_m} m(x) S^*(x, M^*)(\cos(\alpha h(x)) - \mathrm{i}\sin(\alpha h(x)))\,\mathrm{d}x}{1 + \frac{B^*}{K(x, M^*)\alpha} e^{(-\lambda_0 a_h)} \int_{x_h}^{x_m} m(x) S^*(x, M^*)(\sin(\alpha h(x)) + \mathrm{i}(\cos(\alpha h(x)) - 1))\,\mathrm{d}x}. \end{aligned} \tag{50}$$

Then, defining

$$C = B^* \exp(-\lambda_0 a_h) \int_{x_h}^{x_m} m(x) S^*\big(x, M^*\big) \cos\big(\alpha h(x)\big)\,\mathrm{d}x \tag{51}$$

$$S = B^* \exp(-\lambda_0 a_h) \int_{x_h}^{x_m} m(x) S^*\big(x, M^*\big) \sin\big(\alpha h(x)\big)\,\mathrm{d}x, \tag{52}$$

and noting the definition of M^*, we obtain

$$f_{\gamma} = \frac{C - \mathrm{i}S}{1 + \frac{S + \mathrm{i}(C - M^*)}{K(x, M^*)\alpha}} \tag{53}$$

$$= K\big(x, M^*\big)\alpha \frac{(CK(x, M^*)\alpha + SM^*) - \mathrm{i}(SK(x, M^*)\alpha + S^2 + C^2 - CM^*)}{(K(x, M^*)\alpha + S)^2 + (C - M^*)^2}. \tag{54}$$

Hence,

$$\begin{bmatrix} \Re \\ \Im \end{bmatrix} \left(\frac{1 - f_\gamma F_\gamma(x)}{G(x)^\gamma} \right) = \begin{bmatrix} \cos(\alpha h(x)) \\ -\sin(\alpha h(x)) \end{bmatrix} - \begin{pmatrix} a_{11} & a_{12} \\ -a_{12} & a_{11} \end{pmatrix} \begin{bmatrix} \sin(\alpha h(x)) \\ \cos(\alpha h(x)) - 1 \end{bmatrix}, \tag{55}$$

where $a_{11} = [CK(x, M^*)\alpha + SM^*]/A$ and $a_{12} = [SK(x, M^*)\alpha + S^2 + C^2 - CM^*]/A$, where $A = (K(x, M^*)\alpha + S)^2 + (C - M^*)^2$.

Finally, we obtain the two equations

$$\exp(a_h \lambda_0) \begin{bmatrix} \cos(a_h \alpha) \\ \sin(a_h \alpha) \end{bmatrix} = \int_{x_l}^{x_m} \beta(x) S^*\big(x, M^*\big) \begin{bmatrix} \Re \\ \Im \end{bmatrix} \left(\frac{1 - f_\gamma F_\gamma(x)}{G(x)^\gamma} \right) \mathrm{d}x, \tag{56}$$

that must be satisfied for the two unknowns α and the control parameter (yet to be given).

The starred quantities are known from calculation of the non-trivial equilibrium solution, and C and S are functions of α as defined in Eqs. (51) and (52), respectively. The function $\beta(x)$ is the birth kernel, $m(x)$ is the kernel for M, $K(x, M^*)$ is a function from the death rate defined in Eq. (49), and $h(x)$ is related to the known growth function, $g(x)$, as in Eq. (46).

With the definitions in Sect. 3, a computation reveals that $K(x, M^*)$ now simply equals the constant K_0, and $h(x)$ is computed from Eq. (46) to be $h(x) = g_2(\frac{1}{x_m - x} - \frac{1}{x_m - x_h})$.

Appendix B: Numerical Scheme

The simulation of the model equations is made with a numerical method that integrates the equations along characteristic curves and uses a representation formula of the solution. See Bees et al. (2006) for full details. The method was further adapted to the new system with a boundary delay, which represents the egg stage, and employs a moving grid method with node selection as developed in Angulo and López-Marcos (2004). We briefly document the method here for completeness. For each time, the grid nodes and the approximations to the solution at these points are calculated by means of a characteristics method, except for slugs of minimum size, which are obtained by means of the boundary condition. The formula we use in the numerical method is based upon a theoretical integration along characteristics, which provides the next representation of the solution to problem (19). Hence,

$$s\big(t, x(t; t_*, x_*)\big) = s(t_*, x_*) \exp\left(- \int_{t_*}^{t} \mu^*\big(x(\tau; t_*, x_*), M(\tau), \Pi(\tau)\big)\, \mathrm{d}\tau \right), \tag{57}$$

where $\mu^*(x, M(t), \Pi(t)) = \mu(x, M(t), \Pi(t)) + g'(x)$, and $x(t; t_*, x_*)$ is the solution of

$$\begin{cases} \dfrac{dx}{dt} = g\big(x(t)\big), \\ x(t_*) = x_*. \end{cases} \tag{58}$$

Given positive integers R and J with a fixed time interval $[0, T]$, we define $\Delta t = a_h/R$, $\Delta x = (x_m - x_h)/J$ and $N = [T/\Delta t]$, with $N+1$ discrete time levels $t_n = n\Delta t$, $0 \le n \le N$. The initial grid nodes are chosen as $X_j^0 = x_h + jh$, $0 \le j \le R$, with the numerical initial condition (equal to the theoretical initial condition at each node) $U_j^0 = s(X_j^0, 0)$, $0 \le j \le J$. The initial condition for a delay problem requires a value of the solution for $[-a_h, 0]$. However, the delay appears only at the boundary, so we store eggs laid for each time t, by introducing $L_n = \frac{x_h}{a_h} l(0, t_n)$, where $l(0, t_n)$ represents the eggs laid at $t = t_n$, $-R \le n \le 0$. For the general time step, t_{n+1}, $0 \le n \le N-1$, we assume that the solution approximations and grid at the previous time level t_n are known. Then, defining

$$X_{j+1}^{n+1} = X_j^n + \Delta t g\left(X_j^n + \frac{\Delta t}{2} g\big(X_j^n\big)\right), \quad 0 \le j \le J-1, \tag{59}$$

$$X_{J+1}^{n+1} = X_J^n, \tag{60}$$

$$\begin{aligned} U_{j+1}^{n+1} = U_j^n \exp\Bigg\{-\Delta t \mu^*\Bigg(X_j^n + \frac{\Delta t}{2} g\big(X_j^n\big), \\ \frac{Q(\mathbf{X}^n, \boldsymbol{\gamma}_M^n \mathbf{U}^n) + Q(\mathbf{X}^{n+1}, \boldsymbol{\gamma}_M^{n+1} \mathbf{U}^{n+1})}{2}, \\ \frac{Q(\mathbf{X}^n, \boldsymbol{\gamma}_\Pi^n \mathbf{U}^n) + Q(\mathbf{X}^{n+1}, \boldsymbol{\gamma}_\Pi^{n+1} \mathbf{U}^{n+1})}{2}\Bigg)\Bigg\}, \\ 0 \le j \le J-1, \end{aligned} \tag{61}$$

$$U_{J+1}^{n+1} = U_J^n, \tag{62}$$

we compute

$$U_0^{n+1} = \frac{L_0^{n-R+1} \exp(-a_h \mu_0)}{g(x_h)}, \quad \text{and} \quad L_0^{n+1} = Q\big(\mathbf{X}^{n+1}, \boldsymbol{\beta}^{n+1} \mathbf{U}^{n+1}\big). \tag{63}$$

Here, $\beta_j^n = \beta(X_j^n)$, $0 \le j \le J+1$, $(\gamma_s)_j^n = \gamma_s(X_j^n)$, $0 \le j \le J+1$, $s = M, \Pi$; and $Q(\mathbf{X}^l, \mathbf{V}^l) = \sum_{j=0}^{J+l} q_j^l(\mathbf{X}^l) V_j^l$, $l = 0, 1$, where $q_j^l(\mathbf{X}^l)$, $0 \le j \le J+l$, $l = 0, 1$, are the coefficients of the composite trapezoidal quadrature rules with nodes in $\mathbf{X}^l$. Also, $\boldsymbol{\gamma}_s^n \mathbf{U}^n$, $s = M, \Pi$; and $\boldsymbol{\beta}^n \mathbf{U}^n$, represent the component-wise product of the corresponding vectors, $0 \le n \le N$. Note that the functions γ_s, $s = M, \Pi$, are the kernels of the integrals in the definitions of functions M and Π.

The number of nodes might vary at consecutive time levels as new nodes are introduced to the scheme that flux through node x_h. Therefore, the first grid node X_l^{n+1} that satisfies

$$\big|X_{R+l+1}^{n+1} - X_{R+l-1}^{n+1}\big| = \min_{1 \le j \le J} \big|X_{R+j+1}^{n+1} - X_{R+j-1}^{n+1}\big|, \tag{64}$$

is removed, maintaining a constant number of nodes for each time level involved in the implementation of the step scheme ($(J+2)$ and $(J+1)$ for the current and previous levels, respectively). However, we do not recompute the approximations to

the nonlocal terms at such time levels. The grid (subgrid of the complete system, in which all the nodes take part) is composed of x_h, the minimum size of slugs, together with the nodes obtained by integration along characteristics from the nodes selected at the previous time level. The solutions are defined by an implicit system of equations given by (61), which are solved via an iterative procedure. (This scheme can be easily extended to treat problems where the slug growth function depends additionally on a weighted sum of the population.)

References

Abia, L.M., Angulo, O., López-Marcos, J.C.: Size-structured population dynamics models and their numerical solutions. Discrete Contin. Dyn. Syst., Ser. B **4**, 1203–1222 (2004)

Abia, L.M., Angulo, O., López-Marcos, J.C.: Age-structured population models and their numerical solution. Ecol. Model. **188**, 112–136 (2005)

Abia, L.M., Angulo, O., López-Marcos, J.C., López-Marcos, M.A.: Numerical schemes for a size-structured cell population model with equal fission. Math. Comput. Model. **50**, 653–664 (2009)

Abia, L.M., Angulo, O., López-Marcos, J.C., López-Marcos, M.A.: Numerical study on the proliferation cells fraction of a tumour cord model. Math. Comput. Model. **52**, 992–998 (2010a)

Abia, L.M., Angulo, O., López-Marcos, J.C., López-Marcos, M.A.: Long-time simulation of a size-structured population model with a dynamical resource. Math. Model. Nat. Phenom. **5**, 1–21 (2010b)

Ackleh, A.S., Ito, K.: An implicit finite difference scheme for the nonlinear size-structured population model. Numer. Funct. Anal. Optim. **18**, 865–884 (1997)

Adimy, M., Angulo, O., Crauste, F., López-Marcos, J.C.: Numerical integration of a mathematical model of hematopoietic stem cell dynamics. Comput. Math. Appl. **56**, 594–606 (2008)

Angulo, O., López-Marcos, J.C.: Numerical schemes for size-structured population equations. Math. Biosci. **157**, 169–188 (1999)

Angulo, O., López-Marcos, J.C.: Numerical integration of nonlinear size-structured population equations. Ecol. Model. **133**, 3–14 (2000)

Angulo, O., López-Marcos, J.C.: Numerical integration of autonomous and nonautonomous nonlinear size-structured population models. Math. Biosci. **177–178**, 39–71 (2002)

Angulo, O., López-Marcos, J.C.: Numerical integration of fully nonlinear size-structured population models. Appl. Numer. Math. **50**, 291–327 (2004)

Angulo, O., López-Marcos, J.C., López-Marcos, M.A., Martínez-Rodríguez, J.: Numerical analysis of an open marine population model with spaced-limited recruitment. Math. Comput. Model. **52**, 1037–1044 (2010a)

Angulo, O., López-Marcos, J.C., López-Marcos, M.A., Milner, F.A.: A numerical method for nonlinear age-structured population models with finite maximum age. J. Math. Anal. Appl. **361**, 150–160 (2010b)

Angulo, O., López-Marcos, J.C., López-Marcos, M.A.: Numerical approximation of singular asymptotic states for a size-structured population model with a dynamical resource. Math. Comput. Model. **54**, 1693–1698 (2011a)

Angulo, O., López-Marcos, J.C., López-Marcos, M.A., Martínez-Rodríguez, J.: Numerical investigation of the recruitment process in open marine population models. J. Stat. Mech. Theory Exp. (2011b). doi:10.1088/1742-5468/2011/01/P01003

Angulo, O., López-Marcos, J.C., López-Marcos, M.A.: A semi-Lagrangian method for a cell population model in a dynamical environment. Math. Comput. Model. (2011c). doi:10.1016/j.mcm.2011.12.016.

Bees, M.A., Angulo, O., López-Marcos, J.C., Schley, D.: Dynamics of a structured slug population model in the absence of seasonal variation. Math. Models Methods Appl. Sci. **12**, 1961–1985 (2006)

Bohan, D.A., Bohan, A.C., Glen, D.M., Symondson, W.O.C., Wiltshire, C.W., Hughes, L.: Spatial dynamics of predation by carabid beetles on slugs. J. Anim. Ecol. **69**, 1–14 (2000)

Calsina, A., Saldaña, J.: A model of physiologically structured population dynamics with a nonlinear individual growth rate. J. Math. Biol. **33**, 335–364 (1995)

Carrick, R.: The life history and development of *Agriolimax agrestis* L. and the grey field slug. Trans. R. Soc. Edinb. **59**, 563–597 (1938)

Choi, Y.H., Bohan, D.A., Powers, S.J., Wiltshire, C.W., Glen, D.M., Semenov, M.A.: Modelling *Deroceras reticulatum* (Gastropoda) population dynamics based on daily temperature and rainfall. Agric. Ecosyst. Environ. **103**, 519–525 (2004)

Choi, Y.H., Bohan, D.A., Potting, R.P.J., Semenov, M.A., Glen, D.M.: Individual based models of slug population and spatial dynamics. Ecol. Model. **190**, 336–350 (2006)

de Roos, A.M.: A gentle introduction to physiologically structured population models. In: Tuljapurkar, S., Caswell, H. (eds.) Structured Population Models in Marine, Terrestrial and Freshwater Systems, pp. 199–204. Chapmann-Hall, New York (1997)

Digweed, S.G.: Selection of terrestrial gastropod prey by Cychrine and Pterostichine ground beetles (Coleoptera: Carabidae). Can. Entomol. **125**, 463–472 (1993)

Hunter, P.J., Symmonds, B.V.: The leapfrogging slug. Nature **229**, 349 (1971)

Ito, K., Kappel, F., Peichl, G.: A fully discretized approximation scheme for size-structured population models. SIAM J. Numer. Anal. **28**, 923–954 (1991)

Kostova, T.V., Chipev, N.H.: A model of the dynamics of intramolluscan trematode populations: some problems concerning oscillatory behavior. Comput. Math. Appl. **21**, 1–15 (1991)

Metz, J.A.J., Diekmann, O.: The Dynamics of Physiologically Structured Populations. Lecture Notes in Biomathematics, vol. 68. Springer, Heidelberg (1986)

Murphy, L.F.: A nonlinear growth mechanism in size structured population dynamics. J. Theor. Biol. **104**, 493–506 (1983)

Pollett, M., Desender, K.: Adult and larval feeding ecology in Pterostichus melanarius Ill. (Coleoptera, Carabidae). Meded. Fac. Landbouwwet. Rijksuniv. Gent **50**, 581–594 (1986)

Purvis, G., Bannon, J.W.: Non-target effects of repeated methiocarb slug pellet application on carabid beetle (Coleoptera: Carabidae) activity in winter-sown cereals. Ann. Appl. Ecol. **121**, 401–422 (1992)

Rae, R., Verdun, C., Grewal, P.S., Robertson, J.F., Wilson, M.J.: Review: biological control of terrestrial molluscs using *Phasmarhabditis hermaphrodita*—progress and prospects. Pest Manag. Sci. **63**, 1153–1164 (2007)

Schley, D., Bees, M.A.: Discrete slug population model determined by egg production. J. Biol. Syst. **10**, 243–264 (2002)

Schley, D., Bees, M.A.: Delay dynamics of the slug *Deroceras reticulatum*, an agricultural pest. Ecol. Model. **162**, 177–198 (2003)

Schley, D., Bees, M.A.: The role of time delays in a non-autonomous host-parasitoid model of slug biocontrol with nematodes. Ecol. Model. **193**, 543–559 (2006)

Shirley, M.D.F., Rushton, S.P., Young, A.G., Port, G.R.: Simulating the long-term dynamics of slug populations: a process-based modelling approach for pest control. J. Appl. Ecol. **38**, 401–411 (2001)

South, A.: A comparison of the life cycles of *Deroceras Reticulatum* (Müller) and *Srion intermedius* normand (pulmonata: stylommatophora) at different temperatures under laboratory conditions. J. Molluscan Stud. **48**, 233–244 (1982)

South, A.: A comparison of the life cycles of the slugs *Deroceras Reticulatum* (Müller) and *Arion Intermedius* Normand on permanent pasture. J. Molluscan Stud. **55**, 9–22 (1989)

South, A.: Terrestrial Slugs. Chapman & Hall, London (1992)

Symondson, W.O.C., Glen, D.M., Ives, A.R., Langdon, C.J., Wiltshire, C.W.: Dynamics of the relationship between a generalist predator and slugs over five years. Ecology **83**, 137–147 (2002)

Tucker, S.L., Zimmerman, S.O.: A nonlinear model of population dynamics containing an arbitrary number of continuous structure variables. SIAM J. Appl. Math. **48**, 549–591 (1988)

Wilson, M.J., Glen, D.M., Hamacher, G.M., Smith, J.U.: A model to optimise biological control of slugs using nematode parasites. Appl. Soil Ecol. **26**, 179–191 (2004)

Zavala, M.A., Angulo, O., Bravo de la Parra, R., López-Marcos, J.C.: A model of stand structure and dynamics for ramet and monospecific tree populations: linking pattern to process. J. Theor. Biol. **244**, 440–450 (2007)